Three-Dimensional, Minimum-Time Turns for a Supersonic Aircraft

J. KARL HEDRICK* AND ARTHUR E. BRYSON, JR.†
Stanford University, Stanford, Calif.

The energy-state approximation is applied to minimum-time three-dimensional turns and numerical results are presented, for a particular aircraft capable of speeds up to Mach number two, for: a) increasing energy turns; b) decreasing energy turns; and c) turns with the same initial and final energy, where the change in heading-angle and/or final energy are specified. In general, the altitude, velocity, and bank-angle vary along the minimum-time path and either thrust is a maximum with variable angle-of-attack or thrust is zero with maximum angle-of-attack (e.g., stall angle-of-attack). Charts of bank-angle and altitude are given as functions of energy and heading-angle-to-go. Significant savings in time are obtained compared to turns using simpler implementations such as constant altitude, constant velocity, and/or constant bank-angle. Minimum time slowdown paths with only the final energy specified and minimum time paths with only the change in heading angle specified are also treated. In the latter case, $\alpha = \alpha_{stall}$, and either $T = T_{MAX}$ or $T = 0$.

Nomenclature

C_{D_0} = zero lift drag coefficient
C_{L_α} = lift coefficient curve slope $[dC_L/d\alpha]$
D = drag = $D_o + D_L \sec^2\sigma$
D_L = drag due to lift when $\sigma = 0$ $[\eta W^2/L_\alpha]$
D_o = zero lift drag
E = energy
g = acceleration of gravity
h = altitude
H = Hamiltonian
L = lift
L_α = lift curve slope $[dL/d\alpha] = C_{L_\alpha} qS$
m = mass of aircraft
M = Mach number
q = dynamic pressure = $\frac{1}{2}\rho V^2$
S = area
T = thrust
T_{MAX} = maximum thrust = $T_{MAX}(V,h)$
V = velocity
W = weight
α = angle-of-attack
α_s = angle-of-attack at stall
β = heading angle
η = aerodynamic efficiency factor
σ = bank angle
λ_β = heading angle adjoint
λ_E = energy adjoint
μ_1 = thrust constraint adjoint
μ_2 = angle-of-attack constraint adjoint
μ_3 = altitude constraint adjoint
ρ = density of atmosphere
γ = flight-path angle

Subscripts

$(\ )_o$ = initial value
$(\ )_f$ = final value

Received May 25, 1971; presented as Paper 71-796 at the AIAA 3rd Aircraft Design and Operations Meeting, Seattle, Wash., July 12-14, 1971; revision received October 7, 1971. This research was supported by NASA Grant NgL-05-020-007.

Index category: Aircraft Performance.

* Research Assistant; now Assistant Professor, Arizona State University, Tempe, Ariz.

† Professor of Applied Mechanics, Aeronautics and Astronautics. Fellow AIAA.

Introduction

ONLY in the last few years have optimization techniques been applied to the turning performance of high-speed aircraft. In Refs. 1, 2, and 3 minimum-fuel and minimum-time turns at constant altitude were investigated. Reference 4 discusses three-dimensional minimum-fuel turns. Beebee[5] has used the energy-state approximation to determine minimum-time three-dimensional turns for a hypersonic rocket-powered aircraft. Kelley and Edelbaum[6] have discussed energy-climbs and energy-turns in terms of asymptotic expansions. Boyd and Christie[7] have also made contributions to the study of performance optimization using energy methods.

In Ref. 3 we investigated minimum-time turns when the airplane was constrained to a constant altitude. In this paper we determine the altitude, bank angle and thrust programs which minimize the time to turn through a specified heading angle and reach a specified energy; we treat velocity as a control variable, and, in general, the minimum time paths show a continuously varying altitude program.

Both altitude and velocity are varied by small changes in the flight-path angle γ, which we assume to be small but not zero. Indeed, each changes at the expense of the other as potential and kinetic energy are interchanged. Because the analysis is simpler, velocity has been chosen as a control variable and altitude as an auxiliary variable, determined by the energy and velocity. Conceptually, it is just as easy to consider altitude as the control variable and velocity as an auxiliary variable. Consequently our control charts are often presented in terms of altitude rather than velocity.

For convenience we use energy-height as a state variable rather than energy; energy-height is simply the energy divided by the acceleration due to gravity ($E.H. = E/g$). Energy-height can be interpreted as the altitude the airplane would reach in a zoom climb if all its energy were converted to potential energy.

Equations of Motion and Constraints

Using the energy-state approximation, the equations of motion† for a point mass are

$$\dot{E} = [V(T - D)]/m \tag{1}$$

$$\dot{\beta} = [g \tan(\sigma)]/V \tag{2}$$

† See Fig. 1 for nomenclature.

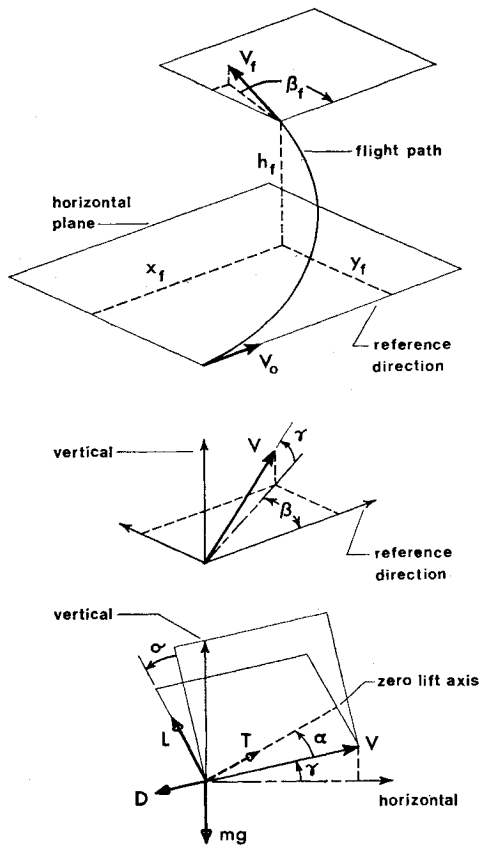

Fig. 1 Nomenclature.

$$\alpha = [W\sec(\sigma)]/L \tag{3}$$

$$h = (E - V^2/2)/g \tag{4}$$

These equations assume that

$|\alpha|$, $|\gamma|$, T/L_α are small compared to unity (5a)

$m \cong \text{const} = m_{\text{average}}$ (5b)

V can be changed instantaneously holding E constant (zoom dives and zoom climbs) (5c)

$|V\dot{\gamma}| \ll g$ (5d)

To make the problem realistic the following constraints were imposed

$$\left.\begin{aligned} \alpha = [W\sec(\sigma)]/L_\alpha \le \alpha_{\text{stall}} &\quad (6a)\\ 0 \le T \le T_{\text{MAX}}(V,h) &\quad (6b)\\ h = (E - V^2/2)g \ge 0 &\quad (6c)\end{aligned}\right\}$$

We have two state variables (E,β), three control variables (T,σ,V), and two auxiliary variables (h,α).

Necessary Conditions

To minimize the turning time we must find the $\sigma(t)$, $T(t)$, and $V(t)$ which minimize t_f, subject to the constraints (1, 2, and 6), as well as

$$\beta(0) = 0 \tag{7a}$$

$$\beta(t_f) = \beta_f \tag{7b}$$

$$E(0) = E_0 \tag{7c}$$

$$E(t_f) = E_f \tag{7d}$$

The variational Hamiltonian for this problem may be written as

$$H = 1 + [(\lambda_\beta g\tan(\sigma)]/V + [\lambda_E V(T - D)]/m + \mu_1 T(T - T_{\text{MAX}}) + \mu_2[([W\sec(\sigma)]/L_\alpha) - \alpha_s] + \mu_3[V - (2E)^{1/2}] \tag{8}$$

where

$$\mu_1\begin{cases} > 0 & \text{if } T = 0, \text{ or } T = T_{\text{MAX}} \\ = 0 & \text{if } 0 < T < T_{\text{MAX}}\end{cases} \tag{9}$$

$$\mu_2\begin{cases} > 0 & \text{if } \alpha = \alpha_s \\ = 0 & \text{if } \alpha < \alpha_s\end{cases} \tag{10}$$

$$\mu_3\begin{cases} > 0 & \text{if } V = (2E)^{1/2} \\ = 0 & \text{if } V < (2E)^{1/2}\end{cases} \tag{11}$$

Necessary conditions for a minimum-time turn include Eqs. (1-4, 6, 7, and 9-11) and the following equations

$$\dot{\lambda}_E = -\partial H/\partial E = (V\lambda_E/m)(\partial D/\partial E) + \mu_1 T\partial T_{\text{MAX}}/\partial E + (\mu_2\alpha_s/L_\alpha)(\partial L_\alpha/\partial E) + \mu_3/(2E)^{1/2} \tag{12}$$

$$\dot{\lambda}_\beta = -\partial H/\partial\beta = 0 \tag{13}$$

$$\partial H/\partial T = \lambda_E V/m + \mu_1(2T - T_{\text{MAX}}) = 0 \tag{14}$$

$$\partial H/\partial\sigma = \sec^2(\sigma)[g\lambda_\beta/V) - (2\lambda_E V D_L\tan(\sigma)/m) + \mu_2 W\sin(\sigma)/L_\alpha] = 0 \tag{15}$$

$$\partial H/\partial V = -[\lambda_\beta g\tan(\sigma)/V^2] + (\lambda_E/m)(\partial/\partial V)[V(T - D)] + \mu_3 - (\mu_1 T\partial T_{\text{MAX}}/\partial V) - (\mu_2\alpha_s/L_\alpha)(\partial L_\alpha/\partial V) = 0 \tag{16}$$

$$\mu_1 \ge 0, \qquad \mu_2 \ge 0, \qquad \mu_3 \ge 0 \tag{17}$$

$$H(t_f) = 0 \tag{18}$$

Since H is not an explicit function of time, a first integral of the optimal turn is $H = \text{const}$; from Eq. (18) this requires that

$$H \equiv 0, \qquad 0 \le t \le t_f \tag{19}$$

Equations (9) and (14) require that

$$\lambda_E = 0 \quad \text{if} \quad 0 < T < T_{\text{MAX}} \tag{20}$$

$$\lambda_E \le 0 \quad \text{if} \quad T = T_{\text{MAX}} \text{ (since } \mu_1 = -\lambda_E V/mT_{\text{MAX}} \ge 0) \tag{21}$$

$$\lambda_E \ge 0 \quad \text{if} \quad T = 0 \text{ (since } \mu_1 = +\lambda_E V/mT_{\text{MAX}} \ge 0) \tag{22}$$

The occurrence of partial thrust can be shown to be very unlikely. From Eqs. (20–22), if $0 < T < T_{\text{MAX}}$ for a finite length of time, then $\lambda_E = 0$ and $\dot{\lambda}_E = 0$; if we rewrite the necessary conditions such that λ_E and $\dot{\lambda}_E$ equal zero, we get the following set of equations

$$1 + [\lambda_\beta g\tan(\sigma)]/V = 0 \tag{23}$$

$$(\mu_2\alpha_s/L_\alpha)(\partial/\partial E)(L_\alpha) + \mu_3/(2E)^{1/2} = 0 \tag{24}$$

$$(g\lambda_\beta/V) + [W\sin(\sigma)/L_\alpha] = 0 \tag{25}$$

$$[g\lambda_\beta\tan(\sigma)/V^2] - \mu_3 + (\mu_2\alpha_s\partial L_\alpha/\partial V)(L_\alpha) = 0 \tag{26}$$

Clearly Eqs. (23–26) cannot be satisfied for μ_2 or $\mu_3 = 0$; i.e., these equations can only be satisfied if we are at sea level with $\alpha = \alpha_s$. Equations (23–26) are also the conditions for a constant energy, constant bank angle turn; it can be shown that a constant energy turn occurs where there is a local maximum

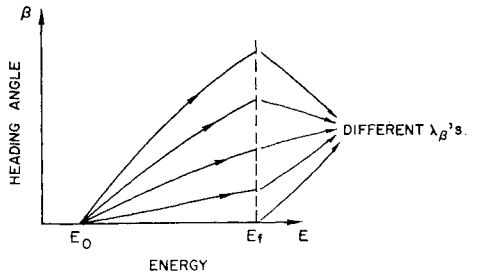

Fig. 2 A one parameter family sketch in the β,E space.

in the $(\dot{\beta})|_{T<T_{MAX}}$ vs Mach number curve. Therefore, the three conditions for a solution involving partial thrust would only be satisfied in the unlikely case that $(\dot{\beta})|_{T<T_{MAX}}$ vs Mach number had a local maximum at a point where $\alpha = \alpha_s$ and $h = 0$. At all other points intermediate values of thrust will not occur, and T will either be zero or T_{MAX}.

If $\alpha < \alpha_s$, then $\mu_2 = 0$, and Eq. (15) requires that

$$\lambda_E = [W\lambda_\beta \operatorname{ctn}(\sigma)/2V^2 D_L] \tag{27}$$

It is clear that $\lambda_\beta < 0$, since $dt_f = \lambda_\beta \delta\beta$, and $\delta\beta > 0$ implies $dt_f < 0$. Hence, from Eq. (27), $\lambda_E < 0$, and, from Eqs. (20–22), this requires that $T = T_{MAX}$.

To develop a set of equations that may be numerically integrated to yield a family of extremals, let us consider the case where $\alpha < \alpha_s$. Substituting Eq. (27) into Eq. (19) we find that

$$\tan(\sigma) = -V/g\lambda_\beta \pm [(V/g\lambda_\beta)^2 - (T_{MAX} - D_0 - D_L)/D_L]^{1/2} \tag{28}$$

Substituting Eq. (28) into Eq. (1) yields

$$\dot{E} = \pm(2VD_L/m)[(V/g\lambda_\beta)^2 - (T_{MAX} - D_0 - D_L)/D_L]^{1/2} \tan(\sigma) \tag{29}$$

for $\alpha < \alpha_s$, where, the (+) sign in Eq. (29) corresponds to the (−) sign in Eq. (28). Thus the two values of σ obtained from Eq. (28) correspond to $\dot{E} > 0$ [(−) sign] and $\dot{E} < 0$ [(+) sign].

Equations (2) and (29) can be integrated numerically to give a one parameter family of optimal paths in the β, E space (λ_β being the parameter) for $\alpha < \alpha_s$, $V < (2E)^{1/2}$; σ and V are obtained by simultaneous solution of Eqs. (28) and (16) where $\mu_2 = \mu_3 = 0$ and μ_1 is given by Eq. (14) with $T = T_{MAX}$, i.e.,

$$\mu_1 = -\lambda_E V/mT_{MAX} \tag{30}$$

If $\alpha < \alpha_s$ but $V = (2E)^{1/2}$ (i.e., $h = 0$), then Eq. (28) gives σ directly and Eq. (16) yields μ_3, still with $\mu_2 = 0$ and μ_1 given by Eq. (30). μ_3 must be > 0; if $\mu_3 \to 0$, climbing begins, i.e., $V < (2E)^{1/2}$ or $h > 0$.

If $\alpha = \alpha_s$ and $V < (2E)^{1/2}$, then $\mu_3 = 0$ and Eqs. (1) and (2) can be integrated numerically with λ_β as a parameter where σ,V, and T are obtained by simultaneous solution of Eq. (16) and

$$\sigma = \cos^{-1}[W/(L_\alpha \alpha_s)] \tag{31a}$$

$$T = \begin{cases} 0; & \lambda_E > 0 \\ T_{MAX}; & \lambda_E < 0 \end{cases} \tag{31b}$$

$$\mu_1 = V|\lambda_E|/mT_{MAX} \tag{31c}$$

$$\mu_2 = (W \sin\sigma/L_\alpha)[(2\lambda_E VD_L \tan\sigma/m) - (g\lambda_\beta/V)] \tag{31d}$$

$$\lambda_E = -(V + \lambda_\beta \tan\sigma)/V^2(T - D) \text{ [from Eq. (19)]} \tag{31e}$$

where μ_2 must be > 0.

Given E_o and $\beta(0) = 0$, we may generate a field of extremals by varying λ_β continuously. A qualitative sketch is given in Fig. 2. Thus, given E_o, E_f, and $\Delta\beta$, we must find the λ_β that will generate a path which satisfies the desired end conditions.

Numerical Results for Minimum Time Turns with Final Energy and Final Heading Angle Specified

The numerical results presented here are for the F4H aircraft whose thrust and aerodynamic characteristics are given in Ref. 9. Minimum-time turns for a particular aircraft, at a given weight, can be presented on two control charts (V or h vs E, σ vs E) and a state space chart ($\Delta\beta$ vs E), all using λ_β as a parameter. The control charts can also be presented as h vs M and σ vs M.

Figure 3 is a plot of altitude vs Mach number and shows that after take-off the airplane accelerates at sea level to approximately $M = 0.86$. At this point the begin-climb condition is satisfied, and the airplane climbs at a nearly constant Mach number of 0.93 to an altitude of 35,000 ft and a Mach number of 1.0. All of the climb trajectories have nearly the same Mach number, altitude history. At this point there is a corner or discontinuity in the control variables: a rapid (zoom) dive at constant energy-height to an altitude of 24,000 ft and a Mach number of 1.27. This is followed by a gradually accelerating climb.

The paths moving from right to left in Fig. 3 are paths of decreasing energy. Unlike the paths of increasing energy, their altitude vs Mach number histories are not identical.

The path indexed by $\lambda_\beta = -14.6$ is representative of those paths whose λ_β is less than -12.5; it is a trajectory without a discontinuity in the controls. Starting at $M = 1.9$, $h = 29{,}000$ ft, the altitude and Mach number decrease to $M = 1.4$, alt $= 25{,}000$ ft. At this point an accelerating climb begins, following the general shape of the accelerating paths described previously.

The path indexed by $\lambda_\beta = -7.4$ is illustrative of the behavior of those paths whose λ_β is greater than -12.5. It decelerates at a nearly constant altitude of 17,000 ft to $M = 1.45$, and then climbs to $M = 1.27$, $h = 23{,}000$ ft. At this point a zoom climb to $M = 1.0$, $h = 33{,}000$ ft occurs, followed by a decrease in altitude and Mach number until $M = 0.96$, $h = 23{,}000$ ft; the trajectory then follows a path of increasing energy. Note that the decreasing energy paths experience a zoom climb discontinuity, the increasing energy paths a zoom dive discontinuity.

A group of optimal paths indexed by $\lambda_\beta > -7.4$ include, in the energy range considered, a period of deceleration at sea level which precedes the gradually decelerating climb, the zoom climb and the decelerating dive after which they join the trajectories of increasing energy.

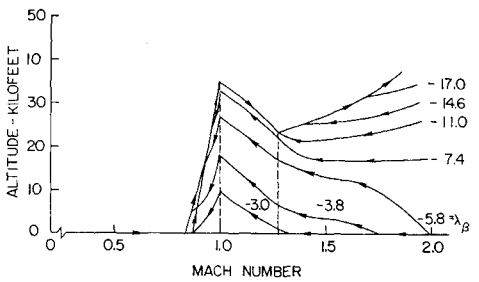

Fig. 3 Altitude for minimum-time turns as a function of Mach number.

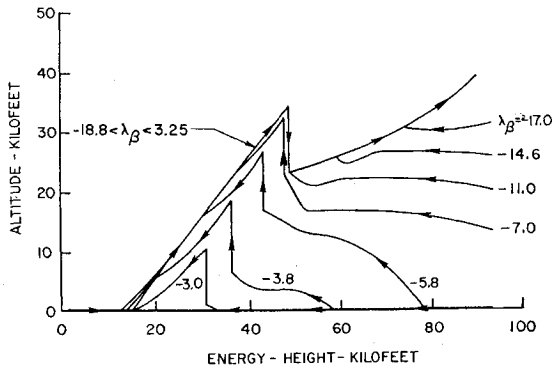

Fig. 4 Altitude for minimum-time turns as a function of energy-height.

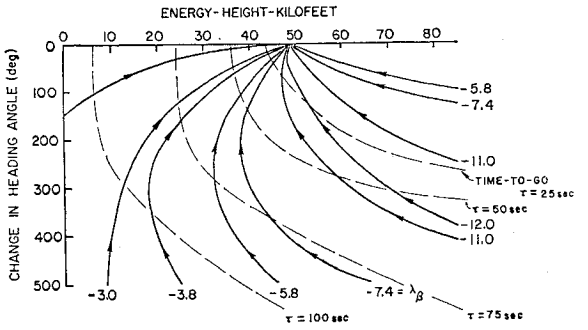

Fig. 6 Change in heading angle for a final energy-height of 49 kft as a function of energy-height with contours of constant time to go.

Figure 4 shows altitude vs energy-height. When compared to Fig. 3, it shows that, although a discontinuity always occurs between $M = 1.0$ and 1.27, it occurs, in the decreasing energy paths, at differing energy-heights. Since the increasing energy paths have nearly the same Mach number-altitude histories, the discontinuity occurs at the same energy-height.

Figure 5 shows bank angle as a function of energy-height. The cross-hatched curve represents the stall boundary. The $\mu_3 = 0$ curve, which intersects each λ_β at the point at which the airplane begins to climb, is represented by the dashed curve that slants upward toward the left. The solid curves represent optimal paths; the directional arrows indicate increasing time. The dashed curve extending horizontally across the graph is the thrust equal drag curve; above this curve the airplane decelerates, below it, it accelerates.

A discontinuity in bank angle occurs at the same energy-height as the discontinuity in altitude shown in Fig. 3. Accelerating paths have a positive jump in bank angle, decelerating paths a negative jump. We can see from Fig. 5 that, in general, there are two basic families of optimal paths; purely accelerating paths at low and intermediate bank angles, and decelerating-accelerating paths at intermediate and high bank angles.

If we wish to reach one particular final energy, we can generate a chart which shows all the paths that end at that energy. Figure 6 is such a chart for a final energy-height of 49 kft, and is typical of charts whose final energy-heights lie in front of the discontinuity in the accelerating paths at 49.5 kft. Figure 6 shows change in heading angle as a function of energy-height. To illustrate how this chart is used, let us consider the case when we wish to turn through 130° and increase our energy-height from 15 kft to 49 kft. Interpolating from Fig. 6, we find that the appropriate λ_β lies between $\lambda_\beta = -1.0$ and $\lambda_\beta = -3.0$ and is approximately equal to -2.0. The trajectory indexed by this λ_β in Figs 4 and 5 gives us the h,σ control program.

Figure 7 is a feedback control chart for a final energy-height of 49 kft. From $E/g = 5$ kft to $E/g = 35$ kft, contours of constant altitude appear as dashed curves, nearly parallel to the state space trajectories. The contours of constant bank angle are represented by the curves, labelled in degrees, between 40° and 85°.

Since a final energy-height of 49 kft was chosen, there are no discontinuities in the controls on the accelerating paths, and 35,000 ft is the maximum altitude attained. However, discontinuities do exist on the slow down paths whenever a trajectory crosses the curve labelled line of discontinuities. The trajectory which begins at $E/g = 65$ kft, $\Delta\beta$ to go = 500°, for example, begins at an altitude of 17,000 ft and a bank angle of 83°. It decelerates and climbs to $E/g \simeq 49.5$ kft, and zoom climbs across the line of discontinuities from 24,000 ft to 35,000 ft. It then decelerates while losing altitude until $E/g = 23$ kft and, finally, accelerates as the bank angle decreases to $E/g = 49$ kft.

For the case when $(E/g)_o = 15$ kft and the desired $\Delta\beta = 130°$, we can determine the bank angle and the altitude programs directly from Fig. 7. We begin at $h = 1{,}000$ ft, $\sigma = 50°$ with an accelerating climb, decreasing the bank angle until $E/g = 49$ kft, $h = 35{,}000$ ft, and $\sigma = 15°$.

Figure 8 shows heading angle as a function of energy-height for all paths whose final energy-height is 60 kft. Since the final energy-height is greater than 49.5 kft, some of the trajectories show a discontinuity in the controls which did not appear in Fig. 7. Some trajectories, having an initial E/g greater than 49.5 kft experience no discontinuities in reaching $E/g = 60$ kft; some trajectories pass through the discontinuity at 49.5 kft and return to 60 kft; two families of trajectories

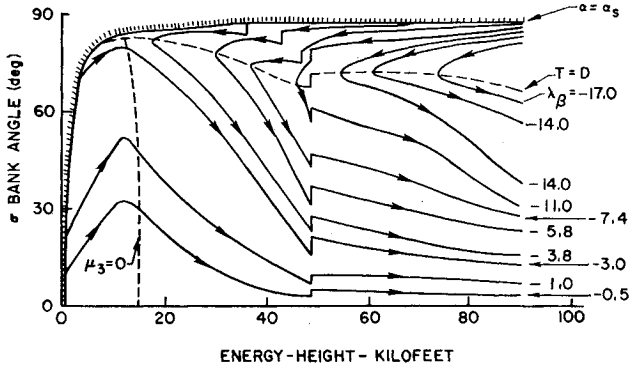

Fig. 5 Bank angle for minimum-time turns as a function of energy-height.

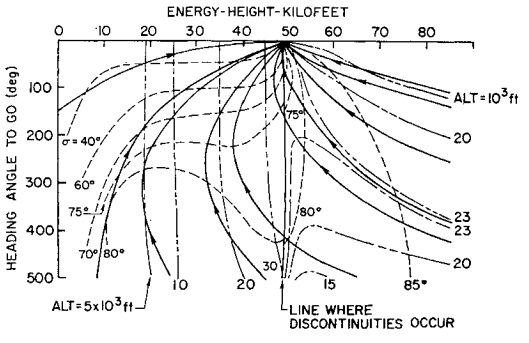

Fig. 7 Feedback control chart for a final energy-height of kft.

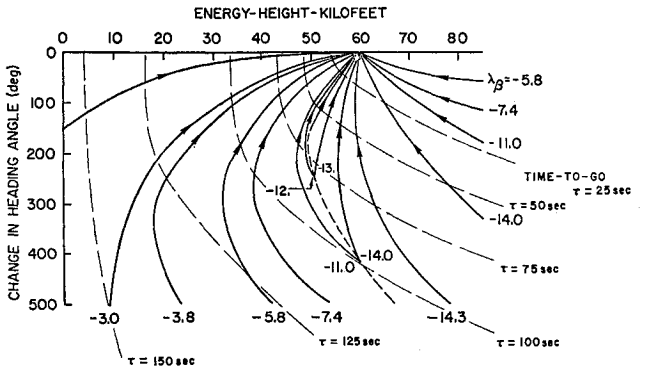

Fig. 8 Change in heading angle for a final energy-height of 60 kft as a function of energy-height with contours of constant time to go.

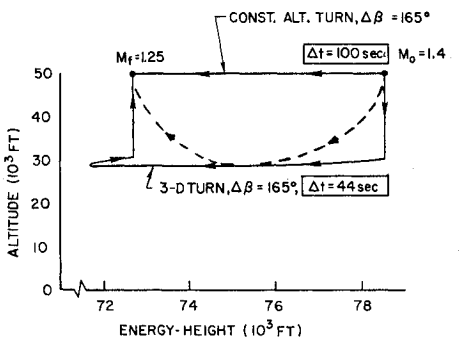

Fig. 10 Altitude programs for 3-D and constant altitude turn (slow down).

overlap in the β vs E/g space. For the latter, the dashed curve represents a contour of constant time which separates these two families. Those trajectories whose initial energy-heights lies on this contour can traverse the same $\Delta\beta$, $\Delta E/g$ on either path in equal time.

Figure 8 is used in the same way as Fig. 6. Given a specific $(E/g)_o$ and $\Delta\beta$, by interpolation we can find the λ_β that will satisfy our required final conditions. Control histories can then be derived from Figs. 4 and 5.

Figure 9 is a feedback control chart for a final energy-height of 60 kft. This chart is further complicated by the discontinuities in control crossing the equal time boundary. This does not affect the trajectories; they never cross an equal time boundary. On the other hand, the contours of constant control do, and must show a discontinuity. This chart is used in the same way as Fig. 8. Given an initial energy-height and a desired $\Delta\beta$, the optimum path can be interpolated; then the bank angle, altitude program can be found from the same figure.

For a complete solution to the three-dimensional minimum-time turn problem, such feedback control charts, covering the full range of possible final energy heights, should be computed.

Comparison of Some Constant Altitude and Three-Dimensional Minimum-Time Paths

In this section a few three-dimensional minimum-time turns will be compared to the corresponding constant altitude minimum-time solutions. Suppose we wish to turn through 165° in minimum time when $(E/g)_o = 78.5$ kft, $(E/g)_f = 72.7$ kft, $M_o = 1.4$, and $M_f = 1.25$, beginning and ending our turn at $h = 50{,}000$ ft. Figures 10 and 11 contain both the constant altitude and the three-dimensional solutions.

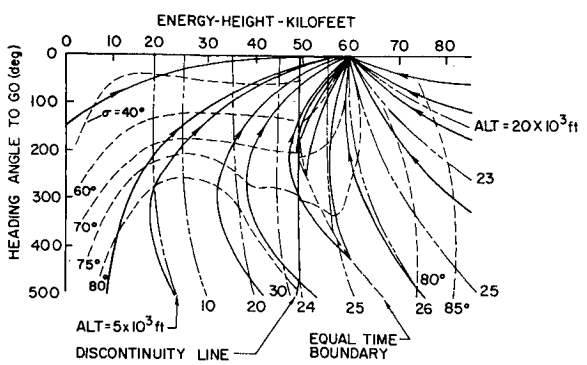

Fig. 9 Feedback control chart for a final energy-height of 60 kft.

The three-dimensional solution begins with a zoom dive from 50,000 ft to 30,000 ft, followed by a nearly constant altitude decelerating turn to an E/g of 71.6 kft. An accelerating climb to $E/g = 72.7$ kft, $h = 31{,}000$ ft is followed by a final zoom climb to the required altitude of 50,000 ft, $M = 1.25$. The bank angle program shown in Fig. 11 decreases steadily from 80° to 67°. The time required to accomplish this 165° turn, assuming instantaneous zoom climbs and dives, is about 44 sec. The constant altitude solution, as shown in Figs. 10 and 11, requires about 100 sec.

For a more accurate solution of the three-dimensional maneuver, we can approximate both the time required to complete the zoom climb and dive and the change in heading angle experienced during them. The 20,000 ft zoom climb and dive should each take about 30 sec to complete, assuming an average speed of 1300 fps and a flight-path angle of about 30°. Since the average turning rate at the optimal altitude is 3.75°/sec and, at the initial altitude is 1.65/sec, an average turning rate of 2.7/sec is reasonable. Using these figures, the entire turn could be accomplished during the zoom dive and climb (60 sec × 2.7°/sec ≅ 165°). Therefore, a four state variable solution would probably have a rounded altitude program such as that described by the dashed lines of Fig. 10, and would require about 60 sec to complete.

A comparison of the three-dimensional and the constant altitude solutions offers some physical insight into the problem. The lower altitude of the three-dimensional solution is the region of maximum specific excess power.[9] Although we want to lose energy while turning, the increase in drag due to lift caused by our extremely high bank angle ($\sigma = 80°$) offers both negative specific excess power and a very high turning rate. If the aircraft were banked this steeply at a higher altitude, it would stall. Similarly, if the thrust were turned off, the desired $(E/g)_f$ would be reached well before the desired turn was completed. It saves time to perform the required $\Delta\beta$ and ΔE simultaneously.

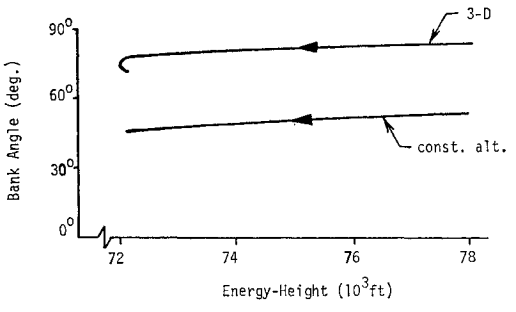

Fig. 11 Bank angle programs for 3-D and constant altitude turn (slow down).

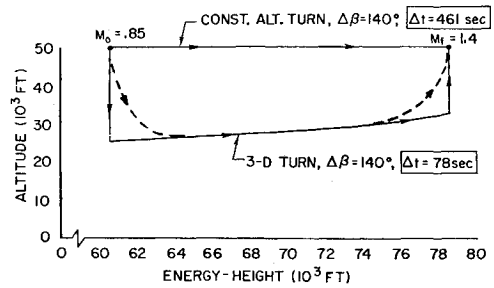

Fig. 12 Altitude programs for 3-D and constant altitude turn (speed up).

The two paths shown in Figs. 12 and 13 go from $(E/g)_o = 60.3$ kft to $(E/g)_f = 78.3$ kft while turning through 140°. The initial and final altitudes are 50,000 ft, and $M_o = 0.85$, and $M_f = 1.4$ In this case the three-dimensional path requires only 78 sec whereas the constant altitude minimum-time path requires 461 sec. Figure 12 shows the altitude program and Fig. 13 the bank angle program for these turns.

If we approximate the time and heading angle change which would occur during the zoom maneuvers, we find that the climb would require 50 sec to perform with a change in heading angle of 50°, the zoom dive 30 sec with a change in heading angle of 30°. Using these approximations,§ the 140° turn would take 110 sec to complete, and the three-dimensional solution is still far superior to the constant altitude solution. The four state variable solution would probably have a rounded altitude program such as that described by the dashed lines in Fig. 12.

As in the preceding example, the three-dimensional speed-up turn occurs at the altitude of maximum specific excess power for wings level flight. Although the high-bank angle causes a decrease in the specific excess power, at this altitude we can maintain our high turning rate without loss of energy. Banking this steeply at 50,000 ft, the specific excess power would be negative. For all increasing energy turns the aircraft should go to the altitude of maximum specific excess power for wings level flight as soon as possible and bank steeply. This results in a high $\dot{E}$ and $\dot{\beta}$.

Minimum-Time Turns with Only Final Energy Specified

Occasionally we are concerned only with increasing or decreasing energy as quickly as possible without regard to the change in heading angle of the airplane. If we wish to increase energy, we want to maximize thrust and minimize drag; to do this, it can be shown that $\lambda_\beta = 0$, $\sigma = 0$, $T = T_{MAX}$ satisfies Eqs. (9–18). Therefore, from Fig. 4, which shows the altitude as a function of energy-height, we should follow the path of increasing energy.

If the initial energy is greater than the desired final energy, we should keep T equal to zero, and maximize our drag. In this case the necessary conditions are satisfied when $h = 0$, $\alpha = \alpha_s$. σ can be found from the equation

$$\sigma = \cos^{-1}(W/L_\alpha \alpha_s)|_{h=0} \tag{32}$$

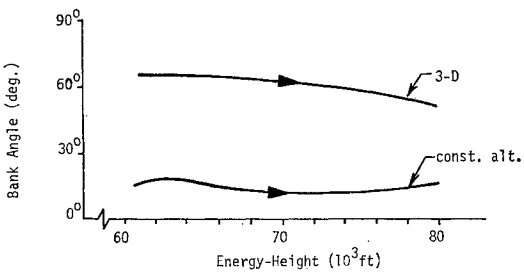

Fig. 13 Bank angle programs for 3-D and constant altitude turn (speed up).

§ The results predicted by the energy-state method are more accurate when changes in altitude due to zoom climbs and dives are small compared to the length of the total flight path.

Minimum-Time Turns with Only Final Heading Specified

If the final energy is not specified, a necessary condition is that $\lambda_E(t_f) = 0$; Eqs. (18, 14 and 15) become

$$\text{at } t = t_f \begin{cases} 0 = [1 + \lambda_\beta g \tan(\sigma)]/V & (33) \\ 0 = (g\lambda_\beta/V) + [\mu_2 W \sin(\sigma)/L_\alpha] & (34) \\ 0 = [-\lambda_\beta g \tan(\sigma)/V^2] - [\mu_2 \alpha_s/L_\alpha][\partial L_\alpha/\partial V] + \mu_3 & (35) \end{cases}$$

Clearly Eqs. (33–35) cannot be satisfied by $\mu_2 = 0$; hence, from Eq. (10), $\alpha(t_f) = \alpha_s$.

This problem can be interpreted as maximizing $\dot{\beta}$ at each energy. Reference 8 shows that this always occurs at sea level with $\alpha = \alpha_s$. We must now decide whether to use maximum or zero thrust; from Eqs. (20–22), this is determined by the sign of λ_E. Solving for λ_E from Eq. (20), we have,

$$\lambda_E = [m/V(D - T)](1 + [\lambda_\beta g \tan(\sigma)/V]) \tag{36}$$

From Eq. (31)

$$\lambda_\beta = -1/\dot{\beta}(t_f) \tag{37}$$

Substituting Eq. (35) into Eq. (34) we have

$$\lambda_E = [m/\dot{\beta}_f V(D - T)](\dot{\beta}_f - \dot{\beta}) \tag{38}$$

Since $\lambda_E > 0$ corresponds to $T = 0$, and $\lambda_E < 0$ corresponds to $T = T_{MAX}$, it follows that

$$T = \begin{cases} T_{MAX} & \text{if } \dot{\beta} > \dot{\beta}_f \\ 0 & \text{if } \dot{\beta} < \dot{\beta}_f \end{cases} \text{ when } D > T_{MAX} \tag{39}$$

$$T = T_{MAX} \quad \text{when} \quad D < T_{MAX} \tag{40}$$

Conclusions

In general, minimum-time three-dimensional turns require variable altitude, variable bank angle programs and either maximum or zero thrust. There are three types of minimum-time three-dimensional turns: a) purely increasing energy turns; b) purely decreasing energy turns; and c) decreasing-increasing energy turns.

As long as the angle-of-attack is less than the stall angle, all minimum-time three-dimensional turns require maximum thrust. When the final energy is not specified, minimum-time turns are always performed with $\alpha = \alpha_s$ and $T = T_{MAX}$ or $T = 0$.

A significant amount of time can be saved by following three-dimensional paths. Comparisons made with constant altitude minimum-time turns show that more time is saved when the initial and final energies differ.

References

[1] Connor, M. A., "Optimization of a Lateral Turn at Constant Height," *AIAA Journal*, Vol. 5, No. 7, Feb. 1967, pp. 335–338.

[2] Bryson, A. E. and Lele, M. L., "Minimum Fuel Lateral Turns at Constant Altitude," *AIAA Journal*, Vol. 7, No. 3, March 1969, pp. 559–560.

[3] Bryson, A. E. and Hedrick, J. K., "Minimum Time Turns for a Supersonic Aircraft at Constant Altitude," *Journal of Aircraft*, Vol. 8, No. 3, March 1971, pp. 182–187.

[4] Bryson, A. E. and Hedrick, J. K., "Three Dimensional, Minimum-Fuel Turns for a Supersonic Aircraft," AIAA Guidance, Control, and Flight Mechanics Conference, Hempstead, N.Y., Aug. 1971.

[5] Beebee, W., "Time Optimal Co-ordinated Turns Using Energy Methods," Measurement Systems Laboratory Rept, May 1970, MIT, Cambridge, Mass.

[6] Kelley, H. J. and Edelbaum, T. N., "Energy Climbs, Energy Turns, and Asymptotic Expansions," *Journal of Aircraft*, Vol. 7, No. 1, Jan.-Feb. 1970, pp. 93–95.

[7] Boyd, J. R. and Christie, T. P., "Energy Maneuverability Theory and Applications," Paper for 12th Annual Air Force Science and Engineering Symposium, Oct. 1965.

[8] Hedrick, J. K., *Optimal Three-Dimensional Turning Maneuvers for Supersonic Aircraft*, Ph.D. dissertation, 1971, Dept. of Aeronautics and Astronautics, Stanford Univ., Stanford, Calif.

[9] Bryson, A. E., Desai, M. N., and Hoffman, W. L., "The Energy State Approximation in Performance Optimization of Supersonic Aircraft," *Journal of Aircraft*, Vol. 6 Nov.-Dec. 1969, pp. 481–487.

FEBRUARY 1972 J. AIRCRAFT VOL. 9, NO. 2.

External Drag of Fuselage Side Intakes

M. D. DOBSON* AND E. L. GOLDSMITH†
Royal Aircraft Establishment, Bedford, England

Results of experiments designed to measure the external drag associated with varying internal flows of fuselage side intakes are presented. At subsonic speeds, cowl lip radius is found to affect drag at full internal flow but its influence decreases as flow is reduced. Conversely, cowl external profile is of significance in terms of spillage drag but does not influence the full flow drag. For a particular rectangular supersonic intake, the addition of swept endwalls is found to affect both full flow and spillage drags. At supersonic speeds, changes in full flow drag with variation of compression surface geometry are compared with those predicted from consideration of shock geometry changes. For supersonic intakes, spillage drag is found to vary in the manner predicted by calculation but for pitot intakes at $M_\infty = 2.0$, calculation over predicts spillage drag because, it is thought, of benefits which arise from the interaction of the intake shock with the fuselage boundary layer. Using a combination of measurement and calculation, pressure drags have been obtained for simple wedge boundary-layer diverters and for two intake configurations at full flow. These latter are compared with values calculated on the basis of isolated pitot intakes.

Nomenclature

A = area
C_D = drag coefficient
D = drag
h = height
M = Mach number
p = static pressure
q = dynamic pressure
r = radius
Re = Reynolds number
γ = ratio of specific heats
δ_2 = compression surface angle (see Fig. 2b)
θ = angle
Δ = increment

Subscripts

BAL = balance
BASE = model base
C = cowl
D = diverter
e = entry (defined in Fig. 2c)
E = external
f = skin-friction
$(F+C)$ = fuselage plus canopy
h = highlight (defined in Fig. 2c)
i = inlet (defined in Fig. 2b)
I = internal
l = lip (defined in Fig. 2c)
L = local flow conditions external to the fuselage boundary layer
P = pressure
PRE = pre-entry
PRE 0 = pre-entry at full internal flow
R = ramp (defined in Fig. 2b)
SPILL = spillage
W = wave
x = duct internal measuring station
∞ = freestream station

Received January 12, 1971; revision received September 14, 1971. Shortened version of paper ICAS 70–49 presented at the 7th Congress of the International Council of the Aeronautical Sciences, Rome, Italy, September 1970.

Index categories: Aircraft Powerplant Design and Installation; and Aircraft and Component Wind Tunnel Testing.

* Principal Scientific Officer, Aerodynamics Department.

† Senior Principal Scientific Officer, Aerodynamics Department.

Introduction

MULTIMISSION combat aircraft, as their name implies, have to perform efficiently over a wide range of flight speed, engine speed and aircraft attitude. They must be able to operate at sea level at high-subsonic or low supersonic speeds to evade detection, to climb to high altitude for inter-